Combination of silicon microstructures and porous cellulose nanofiber structures to improve liquid-infused-type self-cleaning function

Abstract

Various fine structures and/or low surface energy material coatings have been tried to develop self-cleaning surfaces. The structures are intended for air-trap in their vacant spaces. Liquid-infused-type design, another design, has better performance than the traditional one, however, the life is limited because a special liquid covering the surface drops off easily. Cellulose nanofibers (CNF) have amphiphilic characteristics in addition to the small size, thus the aggregated structure will improve the liquid holding performance. This paper discusses the CNF deposition process on silicon microstructured surfaces and the etching process of the CNF structure to extend the self-cleaning life. The effects of the microstructure design, the CNF concentration and the etching conditions on the morphology and the porosity of CNF structures were made clear. Long-term performance tests were carried out measuring sliding angle (SA) of diethylene glycol after repeated water dash as a load. It was confirmed that durable self-cleaning function was obtained with the combined structure of a highly porous CNF structure and a silicon microstructure.

Highlights

CNF structures deposited on silicon micropillar surfaces have well-controlled morphology, vertical wall or horizontal layer (parallel or perpendicular to pillar direction respectively).

An oxygen plasma etching process was introduced to enhance the porosity of dried CNF structures.

The long-term performance of the liquid-infused-type self-cleaning surfaces was improved significantly with combination of a silicon microstructure and a porous CNF structure.

Keywords: self-cleaning, structured surfaces, liquid-infused surfaces, cellulose nanofibers, porous structures, chemical etching

1. Introduction

Various effective functions can be promoted by structured surfaces, e.g., self-cleaning, catalyst, anti-reflection. Many fine structures and/or hydrophobic treatment have been applied for self-cleaning surfaces [1-3]. Omniphobic surfaces on which droplets of high/low surface tension liquids can slide easily have received great interest because of their importance for broad areas. A fine structure filled with a special liquid (a lubricant) in its vacant space is one of solutions for omniphobicity. The affinity for holding the lubricant includes the capillary force and the chemical affinity of hydrophobic surfaces (Fig. 1a) [4]. Other solution is re-entrant design of fine structures [5]. Despite having many advantages, such as very low contact angle hysteresis, self-healing, the liquid-infused surface has an apparent problem comparing with the solid surface. It is easy drop-off of the lubricant due to external loads or stresses, e.g., different liquids, high shear, high temperature [6-8]. The lubricant loss leads to strong adhesion between external liquids and the surface subsequently the decrease of the self-cleaning performance (Fig. 1b). Improvement of the lubricant retention is critical for long-term operation. Comparing with nanostructures, microstructures have higher strength but the capillary force to retain the lubricant is smaller [6]. Thus combination of a nanofiber structure and a microstructure can be a solution to improve the affinity of the solid structure with the lubricant (Fig. 1a). Then durable liquid-infused-type self-cleaning function can be obtained.

Combination of a silicon micropillar array and a porous cellulose nanofiber structure deposited in vacant spaces between the pillars, is one of such designs. Cellulose nanofibers (CNF), a bio-polymer, with high specific surface area and amphiphilic property can improve the affinity with the lubricant. While the silicon pillars can protect the CNF structure against external loads, e.g. mechanical contact. However, there are no preceding studies relating to the affinity improvement including the deposition process. The problem is large aggregation of CNF due to the meniscus force, strong hydrogen bond and mechanical entanglement between the nanofibers [9-11]. Thus a non-uniform and low surface area CNF structure is obtained. Depositing CNF suspension with applicable concentration on a Si micropillar array with a suitable pillar pitch, rich hydroxyl surfaces can be a solution. CNF and the pillars can be linked by hydrogen bond and mechanical entanglement consequently limiting the aggregation. The uniform CNF layer between the pillars can be formed.

The pillars can reduce the aggregation but the porosity of the CNF structure is limited. To obtain a highly porous CNF structure, many efforts have been made to remove the liquid phase without collapsing

the original network structure [10-14]. Surprisingly, no process for increasing the porosity of CNF structures after the drying processes has been reported. Here we introduce an oxygen plasma etching process for that purpose. Before the etching step, CNF suspension can be deposited many times on the silicon structure to obtain a thick CNF layer. Because CNF is weak for chemical reaction [9], all of CNF structures can be removed by the etching reaction. Thus a low power plasma source is preferable. The suitable etching condition need to be made clear. Using oxygen plasma, large aggregated nanofibers remained while the other parts can be etched. Finally the porous CNF structure can be obtained.

This paper aims to fabricate highly porous CNF-silicon surfaces via the drop deposition of the CNF suspensions on the silicon microstructures and the oxygen plasma etching. The deposition conditions and the etching conditions will be made clear. Effects of the CNF structures with and without the plasma etching on the durable improvement of self-cleaning function will be clarified. Finally, suitably structural designs will be discussed.

2. Experiments

2.1. Structuring and hydrophobizing processes

In order to investigate the effects of the CNF-silicon structures on the performance of liquid-infused surfaces, 2 types of the combined structures were produced using different processes. First, the silicon microstructures were fabricated via photolithography and metal-assisted chemical etching (MACE) as shown in Fig. 2. Photoresist was spin-coated on a silicon substrate. After exposition and development, a regular pattern was produced (d is pillar diameter, p is pillar pitch, Fig. 2a, b). In this work, the diameter of 10 µm was chosen and the pitch was change in a range (20-50 µm). A gold layer was then deposited on the substrate for catalyst (Fig. 2c). After etching in a solution of hydrofluoric acid and hydrogen peroxide (etchant), an array of silicon micropillars was obtained (h is height of pillars, Fig. 2d). Etching conditions (etchant, temperature) were chosen based on our previous works of MACE [6, 15]. CNF structures with high surface area play a main role for lubricant retention, while silicon microstructures limit the aggregation of CNF and protect the CNF structures. Thus a silicon structure with high aspect ratio (ratio of pillar height and pillar diameter) is not necessary. Therefore the etching time of 20 minutes was chosen. The pillar height of 15 µm (aspect ratio=1.5) was fixed in this work. The residue of the Au layer was etched using a solution of nitric acid and hydrochloric acid (Fig. 2e). Before CNF deposition, the substrate was dipped in the piranha solution for cleaning and forming of hydroxyl groups that is essential to produce hydrogen bonds

between CNF and the silicon surface (Fig. 2f) [6]. By changing the pitch while fixing the diameter and the height, deposited CNF structures could be controlled.

Fig. 3 shows schematics of two fabrication procedures used to produce CNF vertical wall between the silicon pillars (Fig. 3a: procedure 1, a simple process) or a porous CNF layer (Fig. 3b: procedure 2). In Fig. 3a, the procedure started with drop deposition of aqueous CNF suspensions (0-0.1 wt%) prepared by diluting a commercial CNF hydrogel (1.14 wt%) made from broad leaf. Then the suspensions were dried at room condition. Vertical walls of CNF (parallel to the pillar direction) between the pillars were formed with suitable condition of the pillar pitch and the suspension concentration. In Fig. 3b, however, ethanol was used as solvent for the dilution rather than water to reduce the meniscus force and the aggregation of CNF (subsequently reduce the drying time) [10-11]. The CNF deposition step was repeated many times (layer by layer deposition) to obtain desired thickness of the CNF layer. The profile of this layer is similar with that of the silicon microstructure. The conditions of this step (the pitch and the concentration) will be explained later. They were chosen via results of the procedure 1. In both procedures, CNF and silicon surfaces were linked by hydrogen bonds shown schematically in Fig. 3b. This layer was then etched using oxygen plasma to obtain the highly porous CNF layer. Low power oxygen plasma (Harrick plasma, RF power) that is usually used for cleaning or activating various substrates was used for etching. In this work, the values of power and flow rate were fixed at the default values following the producer recommendation, only etching time was changed. Etched mass of CNF was measured with a high resolution electric balance.

The originally hydrophilic surfaces of the combined structures were modified by depositing self-assembled monolayer (SAM) of octadecyltrichlorosilane (OTS) [6, 16]. This step was done in a glove box purged with dry nitrogen gas to limit effect of humidity that affects to the formation of the OTS multilayer rather than the monolayer. The OTS solution deposition was used because of its simplicity. The final steps of both are lubricant infusion. Table 1 shows detail conditions for the whole experiments.

2.2. Evaluation of the self-cleaning function

Krytox® 103, a lubricant of vacuum pumps, was used as the infused liquid. Before the evaluation, the modified surfaces were infused with Krytox® 103 via the capillary action. Thickness of the lubricant layer (around 30 µm) was kept constantly for all samples by controlling the volume of the lubricant per a sample. The sample was kept for 4 hours at room condition to obtain full wetting and the uniform lubricant layer.

Initial performance of the liquid-infused surfaces was evaluated by measuring sliding angle of diethylene glycol (DEG, a low surface tension liquid [6]). The easier movement of droplets, the higher cleaning performance. For long-term performance, an original set up with a load assuming rainfall to accelerate the loss of the lubricant was used due to the lack of standardization. Figure 4a shows the schematic. Water from a container was poured on a sample surface through a controllable valve. The water dash procedure includes (1) open the valve, (2) keep for certain time, and (3) close valve. By changing the height of the water container (H) or the potential energy of the dash water, the lubricant loss was accelerated (the open time of the valve was fixed). Preliminary trial and previous studies of drop impact on self-cleaning surfaces [4, 17] were referred to choose the suitable value. In this study, the height of 60 cm (the energy of 0.018 J) was set. The dash process was repeated to a desired number. Fig. 4b, c show photos of a sample before and after 150 times of water dash respectively. Here, lubricant-infused silicon surface (p=50 µm) was used because the lubricant loss area could be observed easily. It was identified (white dot curve, Fig. 4c) due to the difference in reflectance of this area and the other area. Blue arrows indicate flow direction of water poured on the surface (Fig. 4a, c). The sliding angle of DEG was then measured immediately. The change of the SA expresses the long-term performance of the lubricant-infused surfaces.

3. Results and discussions

3.1. Well-ordered CNF-silicon structures

Figure 5 shows scanning electron microscope (SEM) images of the typical structures fabricated using the procedure 1 and the procedure 2. The CNF vertical walls were formed between the silicon micropillars over a wide area (Fig. 5a, b). However, they were dense. Inversely, the porous CNF structure was obtained using the procedure 2 (Fig. 5c, d). The inclined view in Fig. 5d shows clearly a silicon micropillar covered by a web-like structure of CNF (the etching time of 4 minutes). In both cases, surface area of the combined structures was increased comparing with that of their corresponding microstructures. Significant improvement of the self-cleaning function can be expected.

3.2. Typical morphologies of CNF structures–Procedure 1

Fig. 6 shows experimental points and areas with typical morphologies of CNF structures. An experimental point includes data of the pillar pitch (horizontal axis) and the CNF concentration (vertical axis). There were 3 areas of the experimental data with 3 main types of the morphology (Fig. 6a). CNF vertical walls were the first type (Fig. 6b). The second type was a horizontal CNF layer that adhered only

to the top of the pillars (Fig. 6c). The third one, a CNF layer was formed on the top of the pillars, the bottom areas between the pillars and along the pillars. The profile of this layer is similar with that of the silicon structure (Fig. 6d). The morphology of the CNF structures could be well controlled by changing the pitch and/or the concentration. In these types, the morphology type 1 was desired. The reason will be shown later.

Fig. 7 shows schematic representations of these typical morphologies. In case of the morphology type 1 and 2, a part of the CNF structures was between the pillars and the other part adhered to the silicon surfaces. Therefore surface area of the combined structures could theoretically increase and the improvement of the affinity with the lubricant was potential (Fig. 7a, b). In case of the morphology type 3, almost all of the CNF structure adhered to the silicon surface (Fig. 7c). In addition, this CNF structure was dense. Fig. 8 that shows high magnification SEM images of this structure at top pillar area and bottom area (p=25 µm, CNF concentration=0.04 wt%) is the evidence. Thus surface area of the combined structure was almost no increase and the improvement of the affinity was not expected.

Fig. 9 shows effect of the CNF morphology on initial performance of the lubricant-infused combined structured surfaces. The silicon structure was fixed (p=20 µm) and the CNF concentration was changed to control the morphology. Sliding angle of DEG was used to evaluate the performance. With the morphology type 1 or 3, the performance was good and not so much different from that of the lubricant-infused silicon surface (without CNF deposition). In case of the morphology type 3, DEG droplets could not slide down and self-cleaning ability was impossible. Combining with the result shown in Figs. 7 and 8, the morphology type 1 was desired because it was potential to improve the affinity while ensuring the initial performance.

We also changed the drying speed (drying temperature) to control the morphology (Fig. 10). With CNF concentration of 0.06 wt% (p=20 µm), the morphology type 2 was obtained by drying at room temperature, drying speed of 40 µl/hour (Fig. 10b). But the morphology changed to vertical walls (type 1) when increasing the drying speed (160 µl/hour, Fig. 10c). In other cases, non-uniform CNF structures occurred (Fig. 10a, d).

3.3. Porous CNF structures–Procedure 2

The morphology of CNF structures could be well controlled using the procedure 1. But their porosity was limited (Fig. 8). Thus the procedure 2 was considered. A CNF structure with the morphology type 3 is the most suitable in the procedure 2 because a horizontal layer is convenient for the uniform

etching process, and the initial performance of the corresponding liquid-infused surface is preserved (Fig. 9). In addition, higher surface area can be obtained by increasing thickness of the CNF layer. Based on the result of the procedure 1 (Fig. 6), it was easier to obtain this type with larger pitch of the silicon structure and smaller concentration of CNF suspension. Therefore the pitch of 50 µm and CNF concentration of 0.04 wt% were chosen in the procedure 2.

The relation between the CNF layer thickness (before oxygen plasma etching step) and number of repeat of the CNF deposition is shown in Fig. 11. They had nearly linear relationship. Inset schematic shows the definition of the thickness. After 20 times of repeat, the thickness was around 2 micrometer. Fig. 12 shows cross-sectional views of a typical structure (5 times of repeat) with low magnification (Fig. 12a), and high magnification (Fig. 12b, c). The thickness is shown in Fig. 12c.

Fig. 13 shows SEM images of the combined structures with etching time of 0 minute (Fig. 13a, b, c), 2 minutes (Fig. 13d, e, f), 4 minutes (Fig. 13g, h, i). The CNF deposition with 10 times of repeat was used. Without the etching process, a dense CNF layer was obtained (Fig. 13b, c), but the aggregation of CNF was reduced comparing with using water as solvent in the procedure 1 (Fig. 8). Porosity of this CNF layer was increased clearly using the oxygen plasma etching (Fig. 13e, f, h, i). However, it is difficult to make a quantitative evaluation of the porosity because of 3 dimensional form of the CNF layers. Uniformly porous CNF structures were obtained in wide ranges.

Fig. 14 shows schematic explanation of the formation of the porous CNF structure. The CNF suspension that includes not only nanofibers but also fiber fragment and non-fibers is heterogeneous (Fig. 14a). In wet state, CNF has high surface area [9]. After drying step, large aggregation of CNF occurred. Because of using ethanol as solvent, the CNF structure had many initial pores that play a role as open areas for the chemical etching (Fig. 14b). Due to the chemical reaction, small fibers and non-fiber parts were etched while large fiber remained (Fig. 14c).

Fig. 15 shows the relation between the etched mass and the etching time. For convenience of mass measurement, a large number of repeat of the CNF deposition was used (20 times). The etching rate was found around 0.05 mg/min. In this case, longer etching time than 6 minutes led to disappear of the CNF structure (result was not shown here).

3.4. Hydrophobization of the CNF-silicon structures

Here the successful hydrophobization of the combined structures was confirmed by comparing the wettability of the lubricant-infused combined surfaces with and without OTS-SAM. Fig. 16a, c show appearances of dyed DEG droplets when they were dropped on both lubricant-infused surfaces. In case of without OTS modification, the DEG droplet spread a wide area (white dot circle, Fig. 16a). The reason was consider as weak affinity between the lubricant layer and the hydrophilic surface. The lubricant layer was unstable and was infiltrated by the droplet (Fig. 16b). In contrast, with OTS deposition the droplet remained (Fig. 16c) and could slide on the lubricant layer. This was the evidence for the successful modification of the combined surface. The lubricant layer was kept stably because it had strong affinity with the hydrophobic surface (Fig. 16d) [5, 6, 18].

3.5. Durable self-cleaning function of the liquid-infused combined structured surfaces

The water dash process was applied for different types of the lubricant-infused surfaces, CNF wall-silicon microstructure, porous CNF-silicon microstructure, and their corresponding silicon microstructures with different pillar pitches (hereafter, labeled "CNF wall-Si", "Porous CNF-Si", "Si-p20", and "Si-p50"). For CNF wall-Si, the pitch of 20 micrometer and the concentration of 0.04 wt% were used. The pitch of 50 micrometer, 10 times of repeat and the etching time of 4 minutes were conditions to produce Porous CNF-Si. In addition, another type of these surfaces, an ideally flat silicon surface with deposited CNF was evaluated to show the effect of the microstructures.

The change of sliding angle after a number of water dash was shown in Fig. 17. After 250 times of water dash, DEG droplets could not slide on the Si-p20 surface and it lost the self-cleaning function. Inversely, the droplets could slide on the CNF wall-Si surface with a large SA (approximate 40°), its function was remained. But the surface became more difficult to clean because the larger inclined angle was required. The CNF wall structure improved the long-term performance of the corresponding silicon structure (p=20 µm), although they had almost same initial performance (curves of Si-p20 and CNF wall-Si). The CNF wall structure improved the long-term performance of the liquid-infused surfaces, however, the effectiveness was limited. Some reasons should be considered. At first, due to small porosity of the CNF layer, the surface area was reduced where this layer wrapped the pillars (Fig. 5a, b) that had high roughness surface [19]. In addition, top of pillars was covered by this dense layer thus there was higher adhesion with DEG droplets. The performance of the CNF-deposited flat surface was evidence for that argument. Without microstructures, DEG droplets could not slide down (Fig. 17, the top left schematic).

Higher effective improvement was obtained using the porous CNF structure. The silicon surface covered with the porous CNF layer (Porous CNF-Si) preserved easy movement of DEG droplets after 250 times of water dash, SA was around 22°. It was easier for movement of DEG droplets on this surface than on the CNF wall-Si surface. After 250 times of dash, the Porous CNF-Si surface was easier to clean than the CNF wall-Si surface. The Si-p50 surface lost its function only after 150 times of water dash. The different results of two microstructures (pitch of 20 µm and pitch of 50 µm) are obvious because the larger pitch structure has smaller capillary force to hold the lubricant.

4. Conclusion

The combined structures of the aggregated CNF and the silicon microstructures were well-controlled. The dense CNF wall structure and the porous CNF structure were obtained with uniformity. And the performance of the liquid-infused self-cleaning surfaces was preserved against large number of water dash, especially with the porous CNF structure.

Producing porous CNF layers with higher thickness that can be used as lubricant reservoir to much enhance the liquid-infused self-cleaning function is one of the future problems. The lubricant retained in the porous CNF layers can be self-refilled to compensate the loss lubricant. More detail discussion about the surface modification of the combined structures produced from two types of material, inorganic material (silicon) and organic material (CNF), should be considered to find the optimal conditions. Scale extension of the surfaces on replicated polymer structures is another future work.
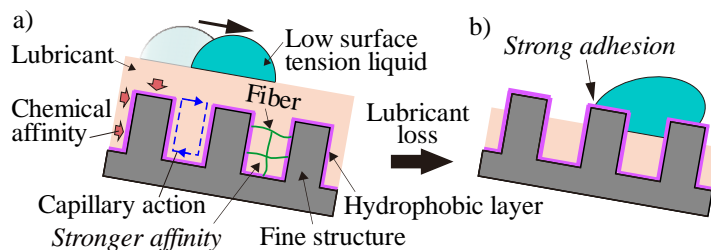
Fig. 1. Liquid-infused-type self-cleaning surface and its problem. a) Lubricant is hold in the fine structure via capillary force and chemical affinity with the hydrophobic layer. Stronger affinity with the lubricant can be obtained with an additional fiber structure [6-7]. b) Drop of low surface tension liquid has strong adhesion with the surface when the lubricant is dropped off and the structure is exposed.
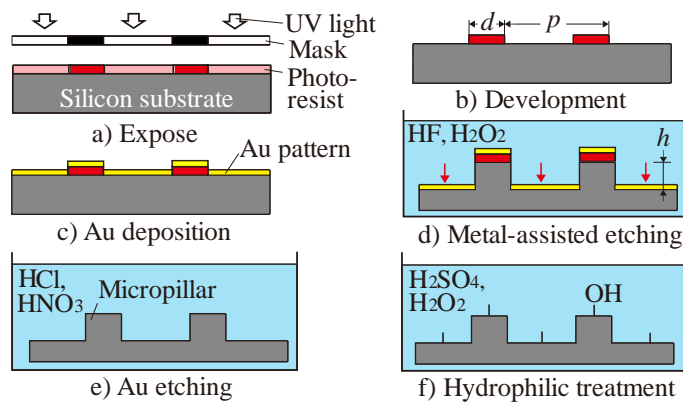
Fig. 2. Fabrication procedure of silicon microstructures. a), b) It started from patterning step of OFPR photoresist on a silicon substrate using the photolithography process. c) An Au layer was deposited to produce an Au pattern. d) The substrate was then dipped in the etchant (a solution of hydrofluoric acid and hydrogen peroxide) and an array of silicon micropillars was fabricated. e), f) Finally, the substrate was dipped in a solution of hydrochloric acid and nitric acid and a solution of sulfuric acid and hydrogen peroxide for Au etching, cleaning, and producing a rich hydroxyl surface.
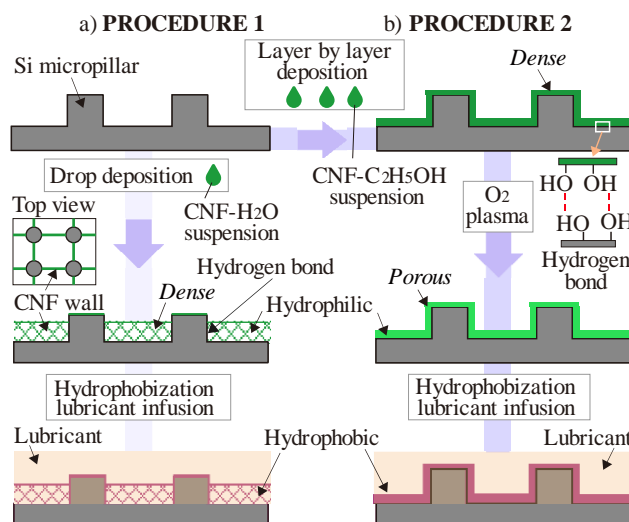
Fig. 3. Fabrication procedures of liquid-infused CNF-silicon surfaces. a) A simple process. CNF suspension was deposited on silicon microstructure surfaces. With a suitable pitch of the microstructures and applicable concentration of CNF, CNF vertical walls (parallel to pillar direction) between the pillars were obtained. b) The CNF deposition step was repeated many times to control the thickness of the horizontal (perpendicular with pillar direction) CNF layer. In both procedures, CNF and silicon surfaces was linked by hydrogen

bonds. The porous structure was then produced using oxygen plasma to increase pore size of the CNF structure. Final step of both procedure is hydrophobization and lubricant infusion.

a) Set up for liquid dash

b) Lubricant-infused silicon surface, (p=50 µm) *before water dash*

c) Lubricant-infused silicon surface, (p=50 µm) *after 150 times of dash*
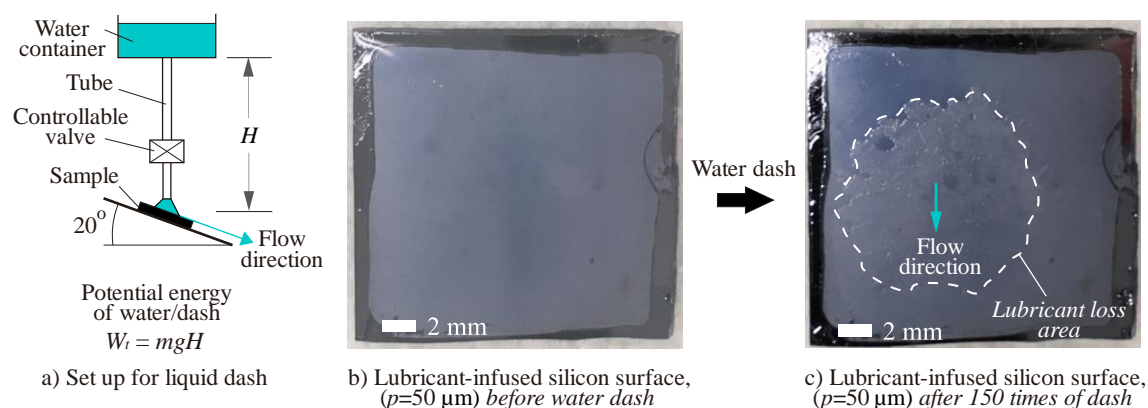
Fig. 4. a) A set up for acceleration of lubricant loss used for durable evaluation. b), c) Photos of a lubricant-infused silicon surface (p=50 µm) before and after 150 times of water dash respectively. The lubricant loss area was identified (white dot curve, Fig. 4c) due to the difference in reflectance of this area and the other area. Blue arrows indicate flow direction of water poured on the surface.

a)-b) Well ordered CNF wall-Si structure **(Procedure 1)**

c)-d) Well ordered porous CNF-Si structure **(Procedure 2)**
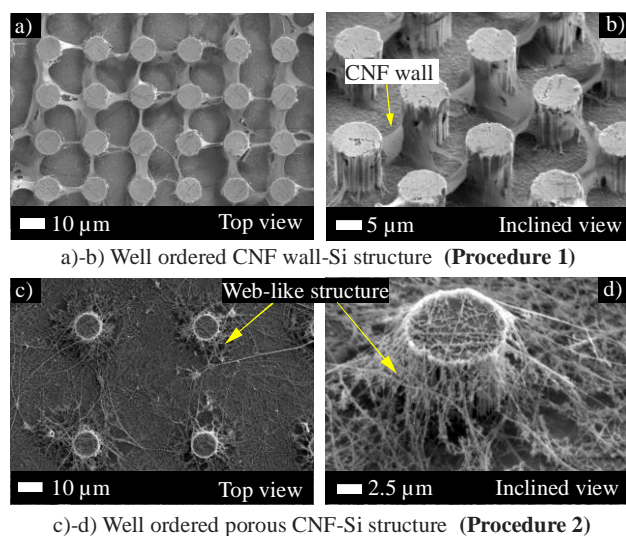
Fig. 5. Well-ordered CNF-silicon structures. a), b) CNF walls were produced between silicon pillars (procedure 1, p=20 µm, CNF concentration of 0.04 wt%). c), d) Highly porous CNF structures were produced on the top of pillar and the bottom area of the silicon surface. Web-like structures of CNF were produced around the pillars (procedure 2, p=50 µm, CNF concentration of 0.04 wt%, number of repeat=10 times, plasma etching time=4 min).

b) Morphology type 1

c) Morphology type 2

a) Experimental points and areas with typical morphologies

d) Morphology type 3

Experimental parameters
d=10 µm, h=15 µm
p=15-50 µm
CNF concentration: 0-0.10 wt%

Evaporation rate: 40 µl/hour
(Room temperature)
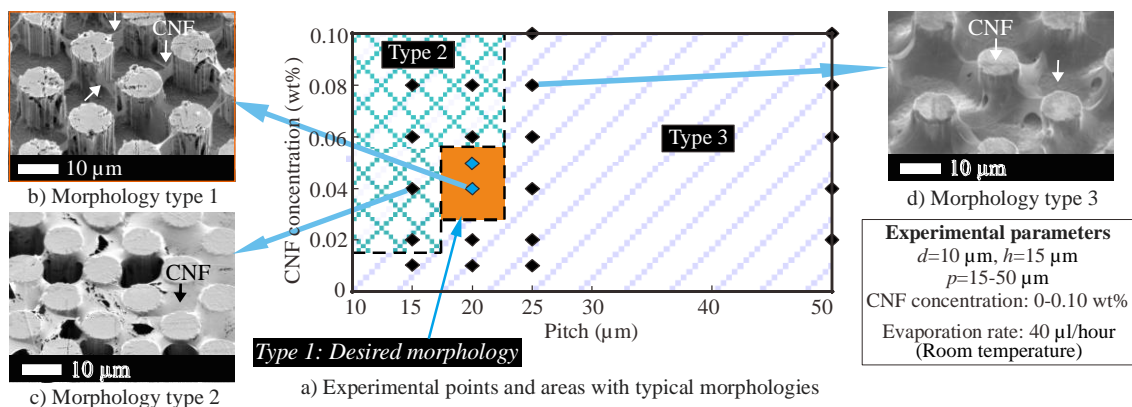
Fig. 6. Deposition of CNF using procedure 1. a) Experimental points and areas with typical morphologies of deposited CNF. An experimental point includes data of the pillar pitch (horizontal axis) and the CNF concentration (vertical axis). b) Morphology type 1 (desired): vertical layer of deposited CNF was formed between silicon pillars. c) Morphology type 2: horizontal layer of deposited CNF was formed on the top of silicon structure. d) Morphology type 3: the profile of this CNF layer is similar with that of the silicon structure. Arrows indicate positions of CNF (b-d).

a) Morphology type 1

b) Morphology type 2
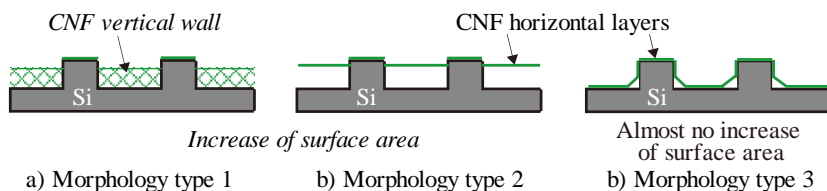
b) Morphology type 3

Fig. 7. Schematic representations of the typical morphologies of CNF deposited using the procedure 1. a), b) CNF structures with morphology type 1 and 2 can theoretically increase surface area of the combined structure and improvement of affinity with the lubricant is potential. c) CNF structure with morphology type 3, surface area of the combined structure is almost no increase.
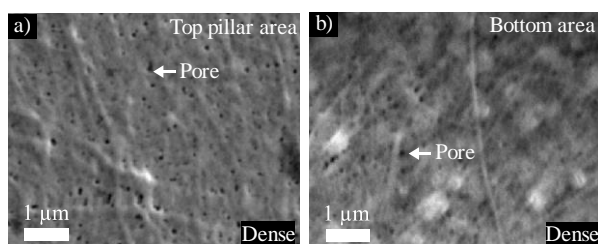
Procedure 1: morphology type 3

Fig. 8. High magnification SEM images of the CNF structure (morphology type 3) fabricated using the procedure 1. a) Top pillar area. b) Bottom surface area (p=25 µm, CNF concentration= 0.04 wt%).
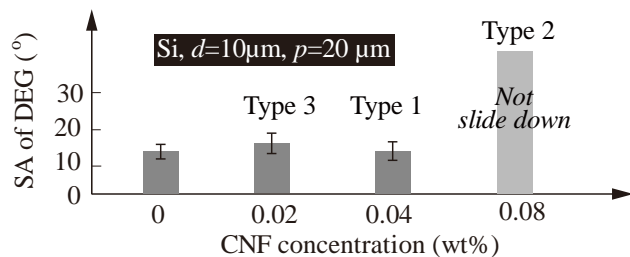

Fig. 9. Initial self-cleaning performance of lubricant-infused surfaces with different morphologies of CNF structure. The performance was measured through sliding angle of DEG. The morphologies were controlled by changing the CNF concentration. Silicon structure (pillar diameter of 10 µm, pitch of 20 µm) is fixed. Error bars indicate standard deviations from at least 3 independent measurements.
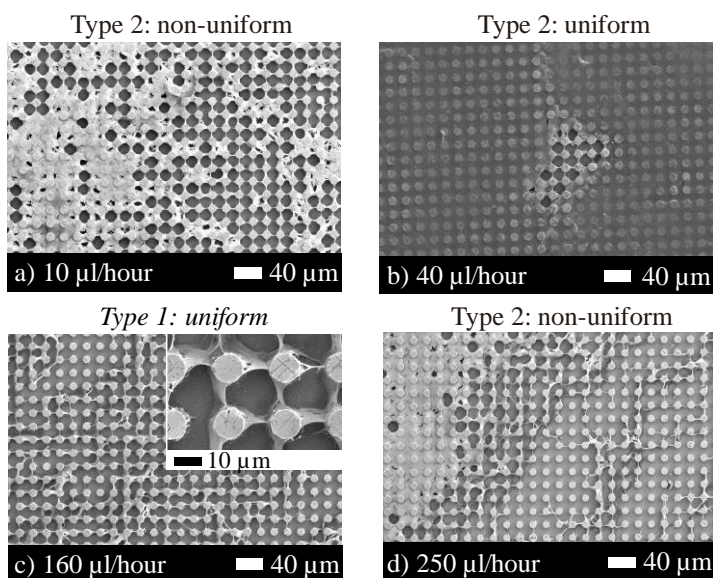
Fig. 10. Procedure1. Effect of evaporation rate on the morphology of CNF structures (p=20 µm, the concentration=0.06 wt%) . a) 10 µl/hour. b) 40 µl/hour. c) 160 µl/hour. d) 250 µl/hour. Uniform CNF vertical wall was obtained with evaporation rate of 160 µl/hour. A uniform, horizontal CNF structure was formed with evaporation rate of 40 µl/hour (drying at room temperature). Non-uniform CNF structures occurred in the other cases.
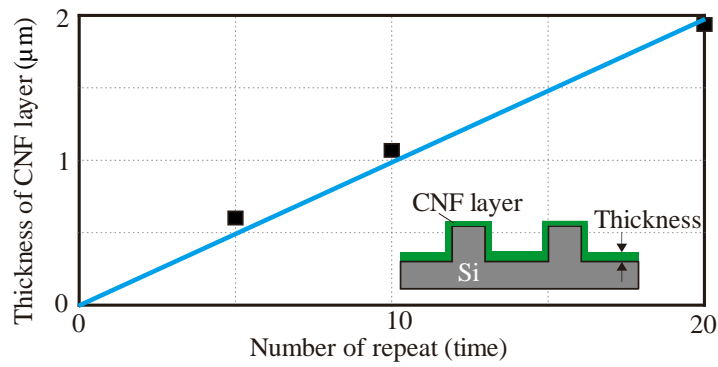
Fig. 11. Relation between the thickness of the CNF layer and number of repeat of the CNF deposition. Inset schematic shows the definition of the thickness (procedure 2, before oxygen plasma etching step).
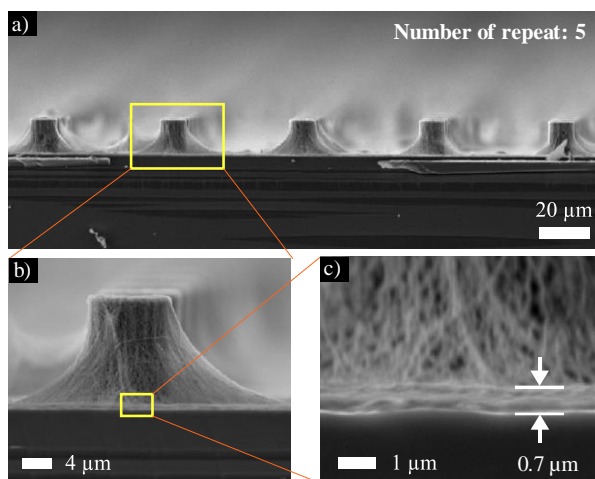

Fig. 12. SEM cross-sectional views of a combined structure (5 times of repeat) with different magnification (procedure 2, before oxygen plasma etching step). a) Low magnification view. b) High magnification view shows one pillar. c) High magnification view shows the thickness of the CNF layer.
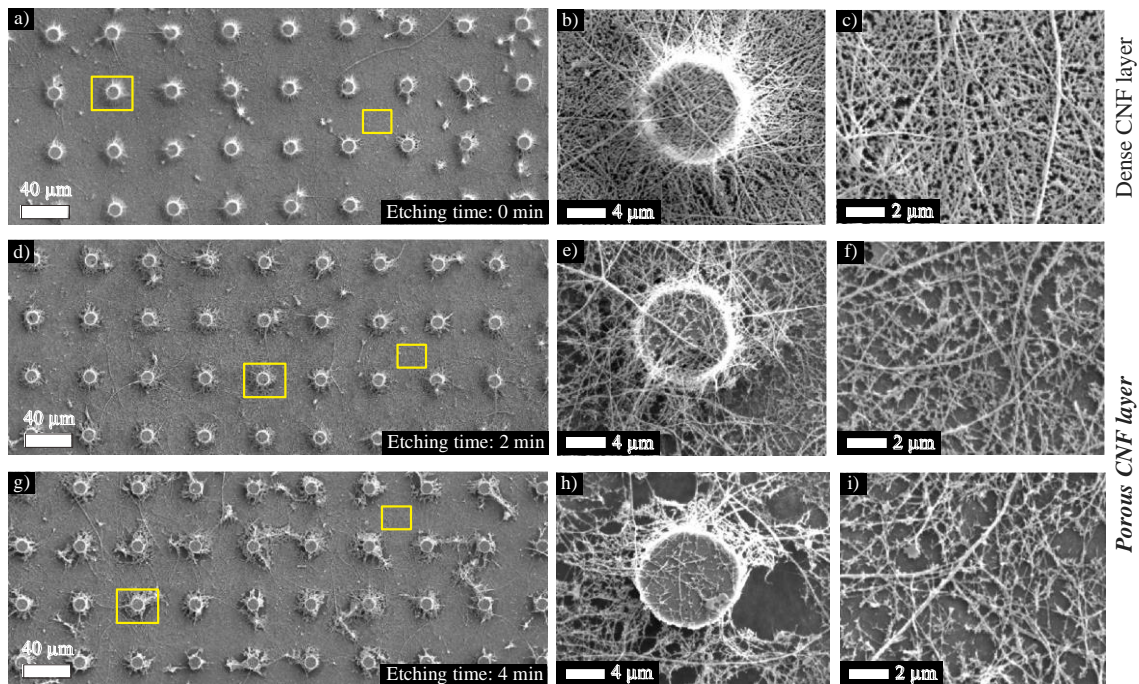
Fig. 13. SEM images of the combined structures with etching time of 0 minute (a-c), 2 minutes (d-f), 4 minutes (g-i). Porous CNF layers were obtained using the oxygen plasma etching. Low magnification views: a), d), g); high magnification views of pillar area: b), e), h); high magnification views of bottom surface area c), f), i). The CNF deposition with 10 times of repeat was used.
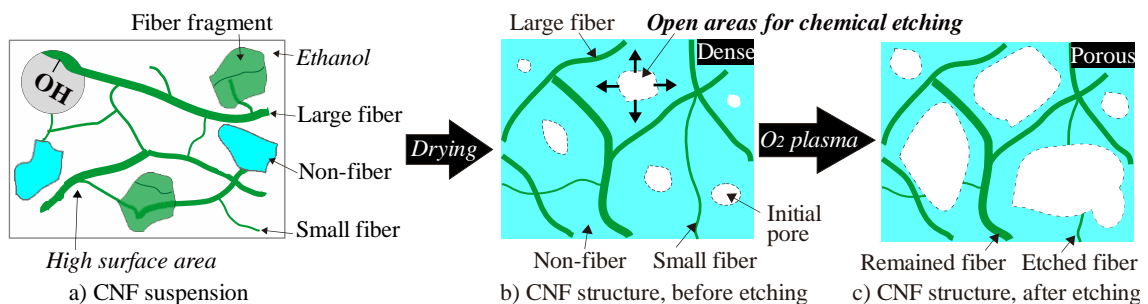

Fig. 14. Schematic explanation of the formation of the porous CNF structure. a) CNF suspension that shows its heterogeneity, rich hydroxyl surface and high surface area of CNF. b) CNF structure, before etching. Large aggregation of CNF occurred when using ambient drying (a simple process, direct transition from liquid phase to gas phase). Because of using ethanol as solvent, the CNF structure had many initial pores that play a role as open areas for the chemical etching. c) CNF structure after etching. Large fibers remained while small fibers and non-fiber parts were etched [9-11].
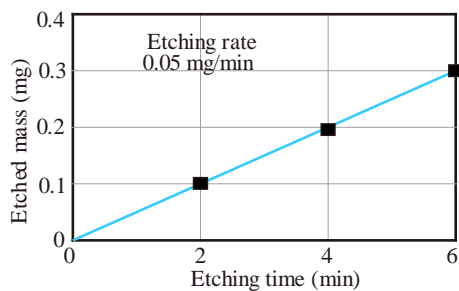
Fig. 15. Relationship between the etched mass and the etching time. 20 times of repeat was used to deposit CNF.
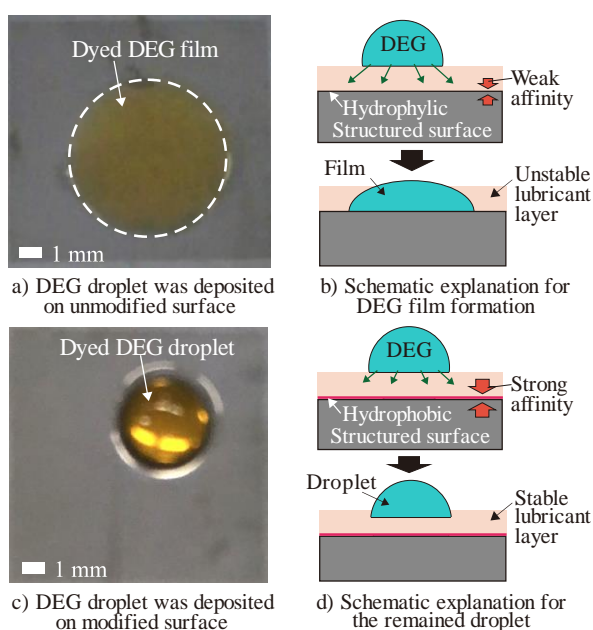

Fig 16. Wettability comparison of the combined surfaces without (a, b) and with OTS modification (c, d). a) A photo (top view) of unmodified surface when a DEG droplet was deposited on it. DEG film was formed (white dot circle). b) Schematic explanation for the film formation. Because of hydrophilicity of the combine surface, it has weak affinity with the lubricant. Thus DEG drop infiltrated to the lubricant layer to form the DEG film and could not slide down at any inclined angle. The lubricant layer was unstable. c) A photo (top view) of a DEG drop when it was deposited on OTS modified surface. The drop was remained. d) Schematic explanation for the remained drop. Because of hydrophobicity of combine surface, it has strong affinity with the lubricant. The lubricant layer was held stably and the DEG drop could not infiltrated to the lubricant layer and could slide down at a suitably inclined angle [4, 19].
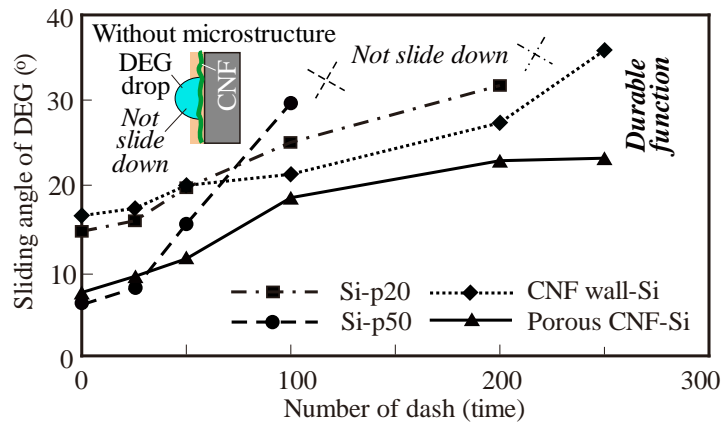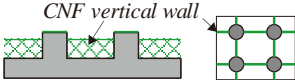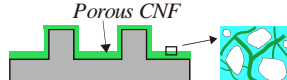
Fig. 17. Durable evaluation. Sliding angle of diethylene glycol measured on 5 types lubricant-infused surfaces. A silicon surface without microstructure (an ideally flat surface) deposited a thin, dense CNF layer (the top left inset). Si-p20: an array of silicon micropillars with pitch of 20 µm. Si-p50: an array of silicon micropillars with pitch of 50 µm. CNF wall-Si: CNF suspension of 0.04 wt% was deposited on an array of silicon micropillars with pitch of 20 µm. Porous CNF-Si: a highly porous CNF layer was formed using 10 times of CNF deposition, the pitch of 50 µm and etching time of 4 min.

Table 1: Detail conditions for fabrication of silicon micropillar structures, deposition of CNF, and hydrophobization.

Substrate material/size		Silicon, 15 mm×15 mm	
Patterning			
Pattern size	d=10 µm, p=15, 20, 25, 50 µm	Expose time	3 sec
Photoresist	OFPR	Development solution, time	NMD3, 10 sec
MACE			
Au layer thickness, deposition method		20 nm, PVD	
Etchant, temperature, etching time, pillar height (h)		HF:H$_2$O$_2$:C$_2$H$_5$OH=3:1:6, 20 °C, 20 min, 15 µm	
Au etching and hydroxylation			
Au etching	Solution, time	HNO$_3$:HCl=1:3, 2 min	
Hydroxylation	Solution, time, temperature	H$_2$SO$_4$:H$_2$O$_2$=3:1, 2 hour, 70 °C	
CNF deposition – Procedure 1		**CNF deposition – Procedure 2**	
CNF vertical wall		*Porous CNF*	
CNF suspension	0-0.1 wt%, Ultrapure water	CNF suspension	0.04 wt%, pure ethanol
Drop volume	200 µl	Drop volume, number of repeat	50 µl, 5-20 times
Evaporation rate	10 µl/hour-250 µl/hour	Evaporation rate	20 µl/min
		O$_2$ plasma, etching time	RF power, 2-6 min
Hydrophobization			
OTS solution, reaction time		3 wt%, anhydrous toluene, 2 hour	